

# THE GENERATION OF STRONG MAGNETIC FIELDS DURING THE FORMATION OF THE FIRST STARS

SHARANYA SUR<sup>1</sup>, D. R. G. SCHLEICHER<sup>2,3</sup>, ROBI BANERJEE<sup>1</sup>, CHRISTOPH FEDERRATH<sup>1</sup>, AND RALF S. KLESSEN<sup>1,4</sup>

*draft November 12, 2018*

## ABSTRACT

Cosmological hydrodynamical simulations of primordial star formation suggest that the gas within the first star-forming halos is turbulent. This has strong implications on the subsequent evolution, in particular on the generation of magnetic fields. Using high-resolution numerical simulations, we show that in the presence of turbulence, weak seed magnetic fields are exponentially amplified by the small-scale dynamo during the formation of the first stars. We conclude that strong magnetic fields are generated during the birth of the first stars in the universe, potentially modifying the mass distribution of these stars and influencing the subsequent cosmic evolution. We find that the presence of the small-scale turbulent dynamo can only be identified in numerical simulations in which the turbulent motions in the central core are resolved with at least 32 grid cells.

*Subject headings:* cosmology: theory — early universe — magnetic fields — turbulence — methods: numerical — stars: formation

## 1. INTRODUCTION

Magnetic fields are ubiquitous in the local universe (Beck et al. 1996) and there is growing evidence of their presence also at high redshifts (Bernet et al. 2008; Robishaw et al. 2008; Murphy 2009). The seeds for these fields are probably a relic from the early universe, possibly arising during inflation or some other phase transition (see, Grasso & Rubinstein 2001; Subramanian 2010, for reviews). Alternatively, they could be generated by astrophysical mechanisms like the Biermann battery (Biermann 1950; Xu et al. 2008) or the Weibel instability (Schlickeiser & Shukla 2003; Medvedev et al. 2004). Regardless of their physical origin, most models predict weak field strengths or have very large uncertainties. Thus, magnetic fields are often ignored in studies of primordial star formation.

However, recent cosmological hydrodynamical simulations of first star formation (Abel et al. 2002; O’Shea & Norman 2007; Yoshida et al. 2008; Turk et al. 2009) show the presence of turbulence in the minihalos where it plays an important role in regulating the transport of angular momentum. This opens up the possibility of exponentially amplifying initially weak seed magnetic fields by the action of the small-scale dynamo. Field amplification via the small-scale dynamo requires both turbulent gas motions and high magnetic Reynolds numbers (Brandenburg & Subramanian 2005).

The properties of the small-scale dynamo have been explored both in numerical simulations of driven turbulence without self-gravity and in analytic models (Haugen et al. 2004; Schekochihin et al. 2004; Brandenburg & Subramanian 2005), as well as in cosmological simulations of magnetic field generation in

galaxy clusters (Xu et al. 2009). The importance of the small-scale dynamo during galaxy formation was previously suggested by Beck et al. (1994), Arshakian et al. (2009), and de Souza & Opher (2010). Its relevance for primordial star formation was previously assessed by Schleicher et al. (2010). Possible amplification mechanisms in the protostellar disk have been previously identified by Pudritz & Silk (1989), Tan & Blackman (2004) and Silk & Langer (2006).

In this Letter, we show, using high resolution numerical simulations that strong and dynamically important magnetic fields are generated from initially weak seed magnetic fields by the small-scale turbulent dynamo during the collapse of primordial halos. The study presented here is a *proof-of-concept* investigation to show that the small-scale dynamo is operational during the collapse of gas clouds, which we apply to the conditions of first star formation. In Section 2 we describe our numerical method and the initial conditions. The results obtained from our numerical simulations are presented in Section 3. Finally, we summarize and discuss our findings in Section 4.

## 2. NUMERICAL METHOD AND INITIAL CONDITIONS

We focus on the gravitational collapse and magnetic field amplification of the baryon-dominated inner parts of a contracting primordial halo, using a simplified initial setup (rather than a full cosmological simulation) where we neglect the detailed thermodynamics and non-ideal MHD effects. The numerical simulations presented here were performed with the publicly available adaptive-mesh refinement (AMR) code, FLASH2.5 (Fryxell et al. 2000). We solve the equations of ideal MHD including self-gravity with a refinement criterion guaranteeing that the Jeans length,

$$\lambda_J = \left( \frac{\pi c_s^2}{G \rho} \right)^{1/2}, \quad (1)$$

with the sound speed  $c_s$  and the gravitational constant  $G$ , is always resolved with a user-defined number of cells. We use an MHD Riemann solver developed for FLASH

arXiv:1008.3481v1 [astro-ph.CO] 20 Aug 2010

<sup>1</sup> Zentrum für Astronomie der Universität Heidelberg, Institut für Theoretische Astrophysik, Albert-Ueberle-Str. 2, 69120 Heidelberg, Germany

<sup>2</sup> ESO Garching, Karl-Schwarzschild-Str. 2, 85748 Garching bei München, Germany

<sup>3</sup> Leiden Observatory, Leiden University, P.O Box 9513, NL-2300 RA Leiden, the Netherlands

<sup>4</sup> Kavli Institute for Particle Astrophysics and Cosmology, Stanford University, Menlo Park, CA 94025, USA

that preserves positive states and proved to be highly efficient and accurate for modeling astrophysical problems involving turbulence and strong shocks (Bouchut et al. 2007; Waagan 2009; Bouchut et al. 2010; Waagan et al. 2010).

The initial conditions for our numerical simulations were motivated from larger-scale cosmological models of Abel et al. (2002), Bromm et al. (2002) and Yoshida et al. (2008). We initialize a super-critical Bonnor-Ebert (BE) sphere with a core density of  $\rho_{\text{BE}} \simeq 4.68 \times 10^{-20} \text{ g cm}^{-3}$  ( $n_{\text{BE}} = 10^4 \text{ cm}^{-3}$ ) at a temperature of  $T = 300 \text{ K}$ . We also include a small amount of rotation of about 4% of the gravitational energy. The radius of the BE-sphere is 1.5 pc which corresponds to a dimensionless radius of  $\xi = 8.28$ . Note that the critical value is 6.451 (Ebert 1955; Bonnor 1956). The total computational domain is  $(3.9 \text{ pc})^3$  in size. The initial conditions are furthermore characterized by the presence of a random initial velocity field with transonic velocity dispersion of amplitude  $1.1 \text{ km s}^{-1}$  (equal to the initial sound speed) and a weak random magnetic field with  $B_{\text{rms}} \sim 1 \text{ nG}$ . This initial field strength corresponds to  $\beta \approx 10^{10}$ , where  $\beta$  is the ratio of the thermal pressure to magnetic pressure. Both, the turbulent energy and magnetic field spectra were initialized with the same power law dependence in wave number space,  $\propto k^{-2}$ , with most power on scales  $\sim 0.8 \text{ pc}$ , which roughly corresponds to the initial Jeans length of the core. Consistent with previous works of Omukai et al. (2005) and Glover & Savin (2009), which follow the thermodynamics during the collapse, we adopt an effective equation of state with  $\Gamma = d \log T / d \log \rho + 1 = 1.1$  for number densities in the range  $n = 10^5 - 10^{10} \text{ cm}^{-3}$ . These initial conditions reflect the physical parameters of the baryon-dominated regime in the centers of the first minihalos (Abel et al. 2002). Hence we can safely neglect the influence of dark matter at this point<sup>5</sup>. The applicability of the ideal MHD approximation for the description of the dynamics has been studied by Maki & Susa (2004) using one-zone models that follow the chemistry, and in particular the abundances of ionized species during the protostellar collapse phase. Their study suggests that the ionization degree is sufficiently high to ensure a strong coupling between ions and neutrals to maintain flux-freezing.

We note that the efficiency of the dynamo process depends on the Reynolds number and is thus related to how well the turbulent motions are resolved (Haugen et al. 2004; Balsara et al. 2004). Higher resolution yields larger field amplification. To demonstrate this effect, we perform five numerical simulations where we resolve  $\lambda_J$  by 8, 16, 32, 64 and 128 cells.

### 3. RESULTS

We find that the dynamical evolution of the system is characterized by two distinct phases. First, as the initial turbulent velocity field decays the system exhibits weak oscillatory behavior and contracts only slowly. Soon, however, the runaway collapse sets in. Fig. 1 shows a

<sup>5</sup> Dark matter would only have an indirect influence on the magnetic field dynamics through its gravitational interaction with the plasma. At low densities, it may accelerate the collapse and introduce additional turbulence in the gas, which could potentially enhance the dynamo.

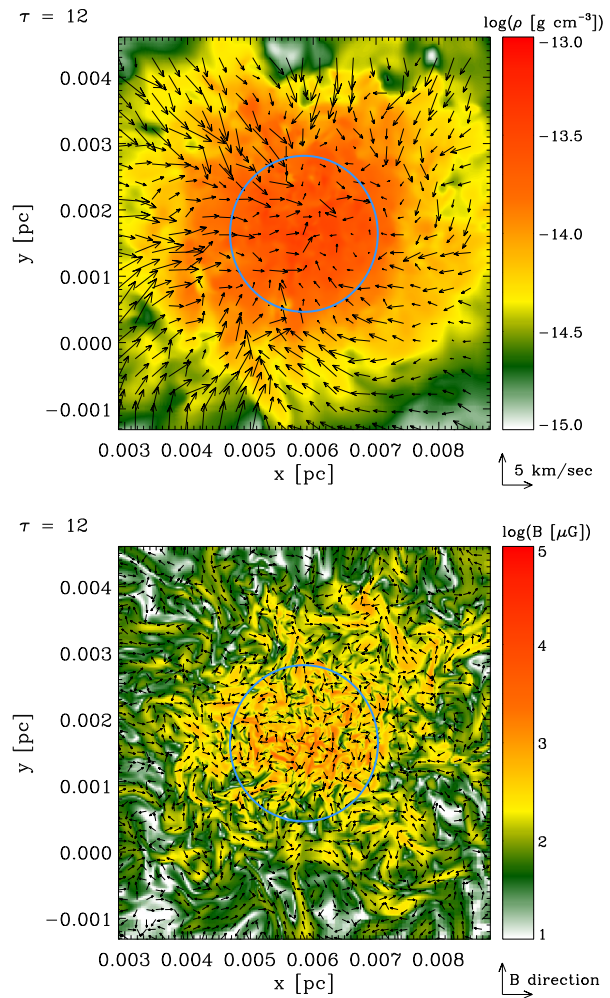


FIG. 1.— Two dimensional slices through the center of the collapsing core at the time when the initial field strength has increased by a factor of  $\sim 10^6$ , showing the central region of our highest-resolution simulation ( $\lambda_J$  resolved by 128 cells). The circle indicates the control volume  $V_J$  centered on the position of the current density peak. The top image shows the density and the velocity component in the  $xy$ -plane, indicating radial infall in the outer regions and turbulent motions in the inner core. The bottom image depicts the total magnetic field amplitude and the local magnetic field direction.

snapshot of the central region of the collapsing core in our highest-resolution simulation at a time when the central density has increased by a factor of  $\sim 10^6$ . The magnetic field strength has grown by a factor of  $10^6$ , reaching a peak value of about 1 mG at  $\tau \sim 12$ . The top image shows the density and the velocity structure, and the bottom image shows the magnetic field strength and the local magnetic field directions.

To understand the behavior of the system more quantitatively, we need to follow its dynamical contraction. First, we note that the physical time scale becomes progressively shorter during collapse. We therefore define a dimensionless time coordinate  $\tau$ ,

$$\tau = \int dt / t_{\text{ff}}(t), \quad (2)$$

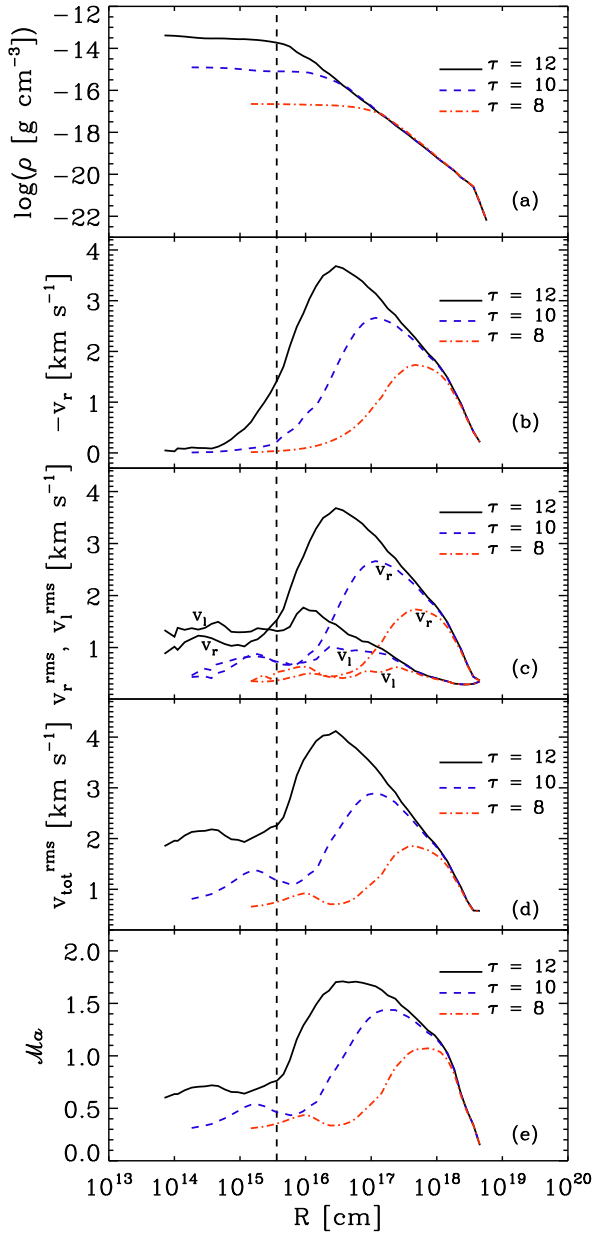


FIG. 2.— Time evolution of the radial density profile (panel a), the radial profile of the mean value of the infall velocity,  $v_r$  (panel b), the radial profile of the rms value of  $v_r$  together with the rms fluctuations of the lateral velocity  $v_l$ , i.e., the component perpendicular to  $v_r$  (panel c), the radial profile of the rms value of the total velocity (panel d) and the Mach number  $\mathcal{M}a$  (panel e). The vertical line indicates the Jeans radius at  $\tau = 12$ . The data are taken from our highest-resolution run.

which is normalized in terms of the local free-fall time,

$$t_{\text{ff}}(t) = \left( \frac{3\pi}{32 G \rho_m(t)} \right)^{1/2}, \quad (3)$$

where  $\rho_m(t)$  is the mean density of the contracting central region. We also define a control volume for gravitational collapse based on the Jeans volume,  $V_J = 4\pi(\lambda_J/2)^3/3$ . We obtain all dynamical quantities of interest as averages within the contracting Jeans volume, which is centered on the position of the maximum density. This approach ensures that we always average over the relevant volume

for collapse and field amplification.

The density profile always maintains a flat inner region within the size of the local Jeans length. This is illustrated in Fig. 2a at three different times, where a flat core of the size of  $\lambda_J$  is sustained throughout the collapse. The radial infall motions dominate the total velocity in the envelope as shown in Fig. 2b. The turbulence is maintained on scales *below*  $\lambda_J$  and dominates the dynamics inside the core region as can be seen from Figs. 2c and 2d, where we show the radial profiles of the magnitude of the fluctuation (rms) value of the infall velocity together with the rms of the lateral component of the velocity and the rms value of the total velocity, respectively. We show in Fig. 2e, the radial profile of the Mach number which illustrates that the infalling velocities are supersonic, while inside the core, the velocities are subsonic.

Gravitational compression during the collapse of a primordial gas cloud can at most lead to an amplification of the magnetic field strength by a factor of  $\sim \rho^{2/3}$  in the limit of perfect flux freezing (i.e., ideal MHD). A stronger increase implies the presence of an additional amplification mechanism. Starting from an initial field strength of  $\sim 1\text{ nG}$ , our simulations show a total magnetic field amplification by six orders of magnitude, leading to a field strength of about  $\sim 1\text{ mG}$  for the case where we resolve the local Jeans length by 128 cells. This is illustrated in Fig. 3a. Fig. 3b shows that in our highest resolution simulation, the obtained field amplification is indeed stronger than what is expected from pure flux freezing, which demonstrates that the small-scale turbulent dynamo provides significant additional field amplification over compression. Fig. 3c shows a plot of the relative amplification in simulations with 16, 32, 64 and 128 cells compared to the simulation where  $\lambda_J$  is resolved by 8 cells, i.e., we divided each curve in Fig. 3b by the curve of the 8 cell run. The time evolution of the mean density  $\rho_m$  within the central Jeans volume is depicted in Fig. 3d, while Fig. 3e shows the plot of the rms velocity. The presence of turbulence delays the collapse until  $\tau \sim 4$ . During this time, the mean density shows oscillations while the rms velocity decreases as the turbulence decays. Sufficient numerical resolution is a crucial issue when studying the small-scale turbulent dynamo. This is evident from Fig. 4, where the simulations with  $\lambda_J$  resolved by 8, 16 and 32 cells are evolved further till  $\tau = 16$ . The 8 and 16 cell runs do not show any increase in  $B_{\text{rms}}/\rho_m^{2/3}$  and only exhibit weak fluctuations, while the 32 cell run is the first to show an increase. This signifies that a minimum of 32 cells per Jeans length is required to obtain the exponential amplification of the magnetic field by the small-scale dynamo. This is also consistent with the turbulence simulations by Federrath et al. (2010), who concluded that at least 30 grid cells are required to resolve turbulent vortices.

As mentioned in Section 2, the growth rate of the magnetic field depends on the Reynolds number of the system and is thus related to the numerical resolution of the simulation. With increasing Reynolds number and thus with higher numerical resolution, the growth rate of the dynamo-generated magnetic field increases (Haugen et al. 2004; Balsara et al. 2004). In agreement with this, our resolution study shows a divergent be-

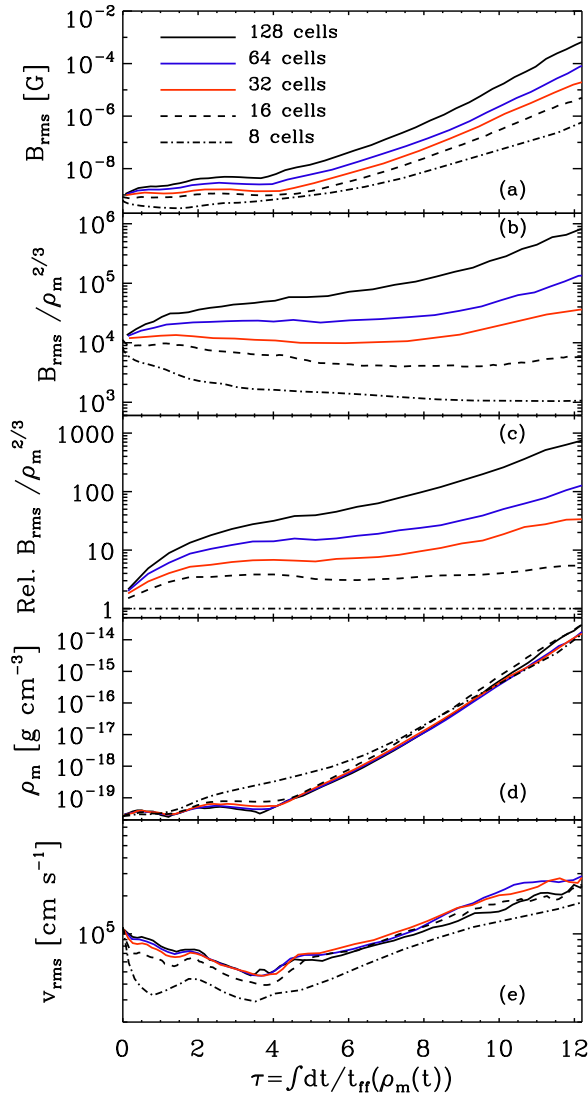


FIG. 3.— Evolution of the dynamical quantities in the central Jeans volume as a function of  $\tau$ , defined in equation (2) for five runs with different number of cells to resolve the local Jeans length. Panel (a) shows the rms magnetic field strength  $B_{\text{rms}}$ , amplified to 1 mG from an initial field strength of 1 nG, (b) the evolution of  $B_{\text{rms}}/\rho_m^{2/3}$ , showing the turbulent dynamo amplification by dividing out the maximum possible amplification due to perfect flux freezing, (c) the relative amplification in  $B_{\text{rms}}/\rho_m^{2/3}$  compared to the 8 cell run, (d) the evolution of the mean density  $\rho_m$  and (e) the rms velocity  $v_{\text{rms}}$ . The runaway collapse commences at about  $\tau \sim 4$ .

havior in the growth rate of the magnetic field (Fig. 3b and 3c) rather than a convergent one. A convergence in the growth rate can only be obtained if the physical length scales that determine the Reynolds number are sufficiently resolved. Our simulations also show no signs of saturation and thus we simply stop the calculation when the numerical cost becomes prohibitively high. In reality, we expect the field amplification to continue until back-reactions either via the Lorentz force (Subramanian 1999; Schekochihin et al. 2004) or via non-ideal MHD effects such as ambipolar diffusion (Pinto & Galli 2008) become important. Calculations of MHD turbulence without self-gravity indicate maximum field strengths within

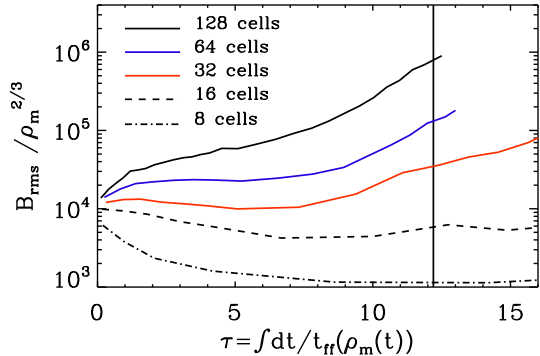


FIG. 4.— The figure illustrates the minimum resolution criterion required to capture the growth of the magnetic field due to small-scale dynamo action. The dynamo begins to be observed for simulations where  $\lambda_J$  is resolved by a minimum of 32 cells. Simulations performed with the Jeans length resolved by either 8 cells or 16 cells are decaying in nature with weak fluctuations. The vertical line indicates the values of  $B_{\text{rms}}/\rho_m^{2/3}$  obtained in the different resolution runs at  $\tau = 12.2$ .

5% of the equipartition value (Subramanian 1999). We note that the physical dissipation scales for ambipolar diffusion and Ohmic dissipation are much smaller than the Jeans length and thus the growth rates obtained in our simulations are lower limits to the physical growth rates.

#### 4. DISCUSSION AND CONCLUSIONS

Studies of primordial star formation show that the gas within the first star forming halos is turbulent (Abel et al. 2002; O’Shea & Norman 2007; Yoshida et al. 2008; Turk et al. 2009). In this Letter, we showed that this turbulence is maintained throughout the collapse and drives a small-scale dynamo, which exponentially amplifies weak magnetic seed fields. We performed five numerical simulations of collapsing Bonnor-Ebert spheres where the local Jeans length was resolved by 8, 16, 32, 64 and 128 cells. Our numerical simulations show that, starting from a weak seed field of  $\sim 1$  nG, strong and dynamically important fields can eventually be generated in the central collapsing core during the formation of the first stars. The small-scale dynamo only works in simulations in which the turbulent motions in the central core are sufficiently resolved. We find that a minimum resolution of 32 cells per Jeans length is necessary for resolving the small-scale dynamo in our simulations.

The generation of strong and dynamically important magnetic fields has interesting consequences for our understanding of how the first stars form and how they influence subsequent cosmic evolution. We know from modeling galactic star-forming clouds that the presence of magnetic fields can reduce the level of fragmentation, and by doing so strongly influences the stellar mass spectrum (Hennebelle & Teyssier 2008). Furthermore, the dynamo-generated strong magnetic fields can drive jets and outflows from the accretion disks via the magnetocentrifugal mechanism (von Rekowski et al. 2003). Such outflows remove a significant fraction of the mass and angular momentum which influences the stellar mass spectrum. The implications of magnetic fields in self-gravitating disks have been explored by Fromang et al.

(2004), who find that the interaction of turbulence excited by the magneto-rotational instability with the self-gravitational instability excites additional modes, broadens the spiral arms and effectively reduces the accretion rate due to non-linear interaction. There are first attempts to study magnetic fields in the context of first star formation (Machida et al. 2006), but more sophisticated initial conditions and more appropriate magnetic field geometries need to be considered.

Once the first stars have formed, they are likely to produce a copious amount of ionizing photons, which drive huge H II regions, bubbles of ionized gas, expanding into the low-density gas between the halos. The effects of radiation have been shown in contemporary star formation (Krumholz et al. 2005, 2007; Peters et al. 2010a,b), and are likely to be important for the first stars as well (Wise & Abel 2008; Greif et al. 2009). The expansion of the H II region could be substantially different if magnetic outflows drive a cavity into the surrounding gas. The magnetic field may further affect fluid instabilities near the ionization front.

The mechanism of exponentially amplifying weak seed magnetic fields via the small-scale dynamo is likely to work not only during the formation of the first stars, but in all types of gravitationally bound, turbulent objects. Highly magnetized gas is thus expected already in the first galaxies.

S. Sur thanks the German Science Foundation (DFG) for financial support via the priority program 1177 'Witnesses of Cosmic History: Formation and evolution of black holes, galaxies and their environment' (grant KL 1358/10). D. R. G. Schleicher is supported by the European Community's Seventh Framework Programme (FP7/2007-2013) under grant agreement No 229517. R. Banerjee is funded by the Emmy-Noether grant (DFG) BA 3607/1. C. Federrath and R. S. Klessen are supported by the Landesstiftung Baden-Württemberg via their program International Collaboration II under grant P-LS-SPII/18. R. S. K thanks the KIPAC at Stanford University and the Department of Astronomy and Astrophysics at the University of California at Santa Cruz for their warm hospitality during a sabbatical stay in 2010. The KIPAC is sponsored in part by the U. S. Department of Energy contract no. DE - AC - 02 - 76SF00515. We acknowledge computing time at the Leibniz-Rechenzentrum in Garching (Germany) and partial support from a Frontier grant of Heidelberg University funded by the German Excellence Initiative. The FLASH code is developed in part by the DOE-supported Alliances Center for Astrophysical Thermonuclear Flashes (ASC) at the University of Chicago.

## REFERENCES

- Abel, T., Bryan, G. L., & Norman, M. L. 2002, *Science*, 295, 93  
 Arshakian, T. G., Beck, R., Krause, M., & Sokoloff, D. 2009, *A&A*, 494, 21  
 Balsara, D. S., Kim, J., Mac Low, M., & Mathews, G. J. 2004, *ApJ*, 617, 339  
 Beck, R., Brandenburg, A., Moss, D., Shukurov, A., & Sokoloff, D. 1996, *ARA&A*, 34, 155  
 Beck, R., Poesz, A. D., Shukurov, A., & Sokoloff, D. D. 1994, *A&A*, 289, 94  
 Bernet, M. L., Miniati, F., Lilly, S. J., Kronberg, P. P., & Dessauges-Zavadsky, M. 2008, *Nature*, 454, 302  
 Biermann, L. 1950, *Zeitschrift Naturforschung Teil A*, 5, 65  
 Bonnor, W. B. 1956, *MNRAS*, 116, 351  
 Bouchut, F., Klingenberg, C., & Waagan, K. 2007, *Numerische Mathematik*, 108, 7  
 —. 2010, *Numerische Mathematik*, 115, 647  
 Brandenburg, A., & Subramanian, K. 2005, *Phys. Rep.*, 417, 1  
 Bromm, V., Coppi, P. S., & Larson, R. B. 2002, *ApJ*, 564, 23  
 de Souza, R. S., & Opher, R. 2010, *Phys. Rev. D*, 81, 067301  
 Ebert, R. 1955, *Zeitschrift für Astrophysik*, 37, 217  
 Federrath, C., Roman-Duval, J., Klessen, R. S., Schmidt, W., & Mac Low, M. 2010, *A&A*, 512, A81+  
 Fromang, S., Balbus, S. A., Terquem, C., & De Villiers, J. 2004, *ApJ*, 616, 364  
 Fryxell, B., Olson, K., Ricker, P., Timmes, F. X., Zingale, M., Lamb, D. Q., MacNeice, P., Rosner, R., Truran, J. W., & Tufo, H. 2000, *ApJS*, 131, 273  
 Glover, S. C. O., & Savin, D. W. 2009, *MNRAS*, 393, 911  
 Grasso, D., & Rubinstein, H. R. 2001, *Phys. Rep.*, 348, 163  
 Greif, T. H., Johnson, J. L., Klessen, R. S., & Bromm, V. 2009, *MNRAS*, 399, 639  
 Haugen, N. E., Brandenburg, A., & Dobler, W. 2004, *Phys. Rev. E*, 70, 016308  
 Hennebelle, P., & Teyssier, R. 2008, *A&A*, 477, 25  
 Krumholz, M. R., Klein, R. I., & McKee, C. F. 2007, *ApJ*, 656, 959  
 Krumholz, M. R., McKee, C. F., & Klein, R. I. 2005, *ApJ*, 618, L33  
 Machida, M. N., Omukai, K., Matsumoto, T., & Inutsuka, S. 2006, *ApJ*, 647, L1  
 Maki, H., & Susa, H. 2004, *ApJ*, 609, 467  
 Medvedev, M. V., Silva, L. O., Fiore, M., Fonseca, R. A., & Mori, W. B. 2004, *Journal of Korean Astronomical Society*, 37, 533  
 Murphy, E. J. 2009, *ApJ*, 706, 482  
 Omukai, K., Tsuribe, T., Schneider, R., & Ferrara, A. 2005, *ApJ*, 626, 627  
 O'Shea, B. W., & Norman, M. L. 2007, *ApJ*, 654, 66  
 Peters, T., Banerjee, R., Klessen, R. S., Mac Low, M., Galván-Madrid, R., & Keto, E. R. 2010a, *ApJ*, 711, 1017  
 Peters, T., Mac Low, M., Banerjee, R., Klessen, R. S., & Dullemond, C. P. 2010b, *ApJ*, 719, 831  
 Pinto, C., & Galli, D. 2008, *A&A*, 484, 17  
 Pudritz, R. E., & Silk, J. 1989, *ApJ*, 342, 650  
 Robshaw, T., Quataert, E., & Heiles, C. 2008, *ApJ*, 680, 981  
 Schekochihin, A. A., Cowley, S. C., Taylor, S. F., Maron, J. L., & McWilliams, J. C. 2004, *ApJ*, 612, 276  
 Schleicher, D. R. G., Banerjee, R., Sur, S., Arshakian, T. G., Klessen, R. S., Beck, R., & Spaans, M. 2010, *MNRAS*, submitted (arXiv:1003.1135)  
 Schlickeiser, R., & Shukla, P. K. 2003, *ApJ*, 599, L57  
 Silk, J., & Langer, M. 2006, *MNRAS*, 371, 444  
 Subramanian, K. 1999, *Phys. Rev. Lett.*, 83, 2957  
 —. 2010, *Astronomische Nachrichten*, 331, 110  
 Tan, J. C., & Blackman, E. G. 2004, *ApJ*, 603, 401  
 Turk, M. J., Abel, T., & O'Shea, B. 2009, *Science*, 325, 601  
 von Rekowski, B., Brandenburg, A., Dobler, W., & Shukurov, A. 2003, *A&A*, 398, 825  
 Waagan, K. 2009, *Journal of Computational Physics*, 228, 8609  
 Waagan, K., Federrath, C., & Klingenberg, C. 2010, *Journal of Computational Physics*, submitted  
 Wise, J. H., & Abel, T. 2008, *ApJ*, 685, 40  
 Xu, H., Li, H., Collins, D. C., Li, S., & Norman, M. L. 2009, *ApJ*, 698, L14  
 Xu, H., O'Shea, B. W., Collins, D. C., Norman, M. L., Li, H., & Li, S. 2008, *ApJ*, 688, L57  
 Yoshida, N., Omukai, K., & Hernquist, L. 2008, *Science*, 321, 669